Microchemical Journal 224 (2026) 117923



Contents lists available at ScienceDirect

Microchemical Journal

journal homepage: www.elsevier.com/locate/microc



Unveiling hidden colors: visualization-augmented deconvolutional SERS (VAD-SERS) for the detection of food colorants and commercial dyes

Yu-Chi Chen [1], Ching-Yu Yu [1], Hsiao-Ju Yu, Jun Hao Wang, Chia-Chi Huang [*]

Department of Chemistry, Tamkang University, No. 151, Yingzhuan Rd., Tamsui Dist., New Taipei City 251301, Taiwan

ARTICLE INFO

Keywords:
Food safety
Colorants
Dyes
Raman scattering
Chromatography
Reversed-phase HPLC

ABSTRACT

We report an innovative and environmentally friendly technique that integrates column chromatography with surface-enhanced Raman scattering (SERS). It works in concert to meet the demand for an economical and intuitive method for color analysis and detecting illegal applications of colorants in food. Alumina powder was modified sequentially to provide dual functions. It is made lipophilic to serve as the stationary phase for reversed-phase liquid chromatography. It is also impregnated with silver nanoparticles (AgNPs) to be a native SERS sensor. This column technology is termed Visualization-Augmented Deconvolutional SERS (VAD-SERS) because it enables the separation and in situ, color-guided SERS detection of individual colorants in a composite color. The effectiveness of VAD-SERS is demonstrated in an experiment that mimics food color adulteration. It is also exhibited in the deconvolution of the color formation in commercial green and brown candies. VAD-SERS is a highly competitive analytical technique, being cost-effective, as efficient as HPLC, easy to set up and operate, and amenable to expansion to preparative scale and the analysis of colorless substances using Raman mapping.

1. Introduction

Color is among the most effective attractants in our world. Food colorants enhance visual appeal and encourage consumption. In nature, many vegetables and fruits evolved to display brilliant colors sustained by active metabolism. After harvesting, however, when the metabolism ceases, the colorants gradually deteriorate. Discoloration can make natural foods lose their appeal or even appear rotten, prompting the often-illegal addition of recoloring agents. For example, the banned Sudan Red [1,2] and Rhodamine B [3] are frequently used on red chili products. Manufactured foods, on the other hand, almost always achieve color appeal through additives. Natural colorants can be extracted and used as additives in manufactured foods, thereby capturing market share by the advertised connection between “natural” and “safe”. However, natural colorants are more expensive while providing fewer color choices than synthetic colorants. Synthetic colorants provide a solution to the color and economic needs. However, many of them have been banned due to potential health risks [4], and additional restrictions are expected according to a recent US FDA resolution to phase out all petroleum-based synthetic dyes from the nation's food supply [5]. Caught in the tug-of-war between near-term manufacturing profits and the long-term costs to consumer health and public trust in the food industry, food producers, consumers, and regulators alike need to be concerned about the analysis of foodborne colors to detect and prevent illegal use of colorants.

Colorimetry is the primary method for colorant analysis. More precise analysis relies on additional techniques, such as chromatography for colorant isolation [6] and an appropriate detection method for determining their structures [7,8]. Specific examples of such integrated techniques include “partial filling micellar electrokinetic chromatography” [9], high-performance liquid chromatography with mass spectrometry (HPLC-MS) [10–12], and nanoparticle-assisted HPLC-UV [13]. These methods are effective but generally require substantial investments in instrumentation, such as a costly ionization method for MS detection of colorant fragments [14,15].

Surface-enhanced Raman scattering (SERS) detects chemical substances by their distinctive sets of molecular vibrations, known as Raman fingerprints. Raman fingerprints characterize molecular structures with a level of specificity similar to nuclear magnetic resonance (NMR) and MS. SERS experiments can be performed either in an aqueous solution or in the solid state with an instrument that costs a fraction of NMR and MS. Unlike NMR and MS, portable Raman

* Corresponding author.
E-mail address: cch@mail.tku.edu.tw (C.-C. Huang).
[1] These authors contributed equally.

https://doi.org/10.1016/j.microc.2026.117923
Received 5 February 2026; Received in revised form 29 March 2026; Accepted 31 March 2026
Available online 2 April 2026
0026-265X/© 2026 Elsevier B.V. All rights are reserved, including those for text and data mining, AI training, and similar technologies.

instruments are readily available for mobile applications if desired [16,17]. SERS has been used to detect food colorants [8,18–22]. These studies focused on SERS substrate development [23–25] and specific hotspot designs [26]. None of them addressed the separation aspect of chemical analysis. An effective separation process for sample treatment ameliorates the selectivity and sensitivity of SERS analysis. Extraction, membrane/capillary electrophoresis, thin-layer chromatography (TLC), and HPLC have been used in combination with SERS as an offline process [27,28]. The development of online SERS detection, particularly in HPLC, is an ongoing pursuit. In addition to the prerequisite of an HPLC system, major restructuring of the SERS process and machinery is necessary to address various challenges, including maintaining a fluid supply of colloidal substrates, the memory effect associated with alternative immobilized substrates, and interference from acetonitrile, the most commonly used mobile-phase component.

In a previous study [8], we developed a solid-state SERS sensor to detect food colorants. The sensor featured isolated hydrophilic niches compartmented by hydrophobic borders on the surface of alumina beads. The hydrophobic borders encouraged silver nanoparticles (AgNPs) and colorant molecules to "slide" into the hydrophilic niches. It facilitated AgNPs aggregation for SERS hotspot formation and increased the local concentration of colorant molecules, thereby improving the detection sensitivity. The sensor was used to analyze the color coating of commercial candies, allowing immediate identification of candy colors rendered with a single colorant. In cases where multiple colorants were used in combination, the SERS spectrum was compared to the composite spectra of individual colorants to provide a close estimate. Here we report the second version of this solid-state sensor, emphasizing improved environmental compatibility and additional separation capability. This technique enables simultaneous separation of colorant mixtures and their visual and SERS identification in a single device. The method is termed visualization-augmented deconvolutional SERS, or VAD-SERS. VAD-SERS not only demonstrates improved SERS sensing but also represents one step closer to an online LC-SERS system.

2. Material and methods

2.1. Material

Deionized ultrapure water (Type I water) with a conductivity of 18.2 MΩ-cm was used in all experiments. Allura Red AC (80% purity), Brilliant Blue FCF (> 97% purity), Sunset Yellow FCF (90% purity), Tartrazine, Indigo Carmine (85% purity), cetyltrimethylammonium bromide (CTAB, ≥ 99% purity), silver nitrate (≥ 99.8% purity), aluminum powder (≤10 μm), sodium citrate tribasic dehydrate were purchased from Sigma-Aldrich. Methylene Blue was purchased from Alfa Aesar. The fluorine-free water repellent (WRP) and industrial dyes were gifts from a local chemical developer. They were used solely for research purposes under the supply agreement. Ethanol (95%) was obtained from Bione Biotech Corp, Taiwan. Acetone was purchased from Macron Fine Chemicals™. Pasteur pipettes were the Duran Wheaton Kimble brand. Color-coated chocolate candies were bought from a local supermarket.

2.2. Fabrication of an aluminum oxide stationary phase

A suspension of citrate-capped AgNPs was prepared as follows. Silver nitrate (27 mg) was dissolved in 150 mL Type I water in a two-neck flask equipped with a condenser. The solution was stirred and heated on a hot plate. The solution temperature was monitored with an infrared thermometer, and an aqueous sodium citrate solution (1% w/vol, 3 mL) was added at 80–83 °C. The reaction was continued in the dark for 1.5 h. It was then cooled to room temperature, and the AgNPs suspension was ready to use.

Aluminum oxide powder (1 or 10 μm diameter, 5.5 g) was incubated with an aqueous solution of CTAB (10^{-4} M, 10 mL) on an orbital shaker for 2 h. The mixture was centrifuged for 2 mins at 424,840*g*, and the supernatant was removed. The precipitate was redispersed in 10 mL of WRP in an oil-in-water emulsion. It was shaken for 2 h before centrifugation and removal of excess WRP. The resultant powder was shaken with citrate-capping AgNPs prepared above (10 mL) for 2 h. The mixture was then centrifuged, and the supernatant was removed. The remaining powder was ready to use after drying at room temperature.

2.3. The production of VAD-SERS columns

A piece of cotton was inserted and placed firmly inside the narrow end of a 15-cm disposable glass Pasteur pipette. Aluminum oxide powder modified as above was mixed with sufficient Type 1 water to form a slurry. A measured amount of this slurry was added to the pipette, and excess water was allowed to drain by gravity. This resulted in a VAD-SERS column of a moistened stationary phase approximately 3 cm in length. The column can be stored in an evacuated zipper bag indefinitely until it fails a test.

2.4. The VAD-SERS process for food colorants and industrial dyes

A 10^{-4} M aqueous solution of selected colorant or dye (200 μL) was loaded onto a VAD-SERS column and allowed to drain by gravity. The column was then eluted with a mobile phase or a gradient of mobile phases consisting of water and acetone (1:0.1 to 1:1 by volume). The flow rate was controlled at approximately 6–7 μL/min using an aquarium air pump. Elution was stopped when the color band of interest had descended an appropriate distance, which required ≤600 μL of mobile phase. Any excess mobile phase was removed from the top. The column was placed horizontally and excited for SERS on a spectrometer.

2.5. The VAD-SERS process for color-coated candies

A piece of candy was immersed in 1 mL of water for 1 min. Then 200 μL of the color liquid was loaded onto a VAD-SERS column. The column was eluted with an appropriate mobile phase. For example, the red candy was eluted with 300 μL 1:1 water-acetone, the yellow candy with 100 μL 1:0.75 water-acetone followed by 100 μL 1:1 water-acetone, the blue candy with 300 μL 1:0.75 water-acetone, the orange candy with 300 μL 1:1 water-acetone, the green candy with 400 μL 1:0.5 water-acetone followed by 50 μL 1:1 water-acetone, and the brown candy with 400 μL 1:0.5 water-acetone.

2.6. Characterizations

Absorption spectra of the citrate-capped AgNPs solutions were recorded on a *V*-730 spectrophotometer (JASCO, Japan). Transmission electron microscopy (TEM) images of AgNPs were recorded using a Hitachi H-7100 TEM system at an accelerating voltage of 75KV (Hitachi, Japan). Field Emission Scanning Electron Microscope (FE-SEM) images of the modified aluminum oxide powder were recorded using a Sigma 300 system with an accelerating voltage of 6 KV (ZEISS, UK). A Raman system (RAMaker, ProTrustTech, Taiwan) equipped with a confocal microscope (100× object lens) and 532 nm laser was used for SERS (conditions: integration time 3 s, cycles 5).

2.7. Chromatography efficiency

The efficiency of column performance within the scope of this study is evaluated using the Theoretical Number of Plates (N) following the United States Pharmacopeia convention [27]:

$N = 16*(M_f/W_b)\hat{}2$

where
N is the theoretical number of plates.

M_f = distance (mm) traveled by the color band from the top of the stationary phase.

W_b = the vertical width (mm) of the developed color band.

2.8. Spectral data processing

The baseline of fluorescence-distorted spectra, if any, was processed for consistent comparison. The method: Given a spectrum represented as a sequence of n + 1 points < (x_0, y_0), (x_1, y_1), …, (x_n, y_n)>, where x_i denotes the number of waves, and y_i represents the intensity. The cubic polynomial regression y = f(x) of the spectrum is used as a baseline. The polynomial regression minimizes the sum of squared error, i.e., $\sum_{i=0,n}(y_i - f(x_i))^2$, ensuring that the baseline extends along the longitudinal center of the spectrum. By removing baseline from the spectrum, an adjusted spectrum <(x_0, y_0-f(x_0)), (x_1, y_1-f(x_1)), …, (x_n, y_n-f(x_n)) > is obtained.

Additionally, to reduce high-frequency noise, an optional smoothing can be performed before the polynomial regression. This involves averaging the intensities over a localized range of wavenumbers. For instance, the smoothed intensity for point y_5 can be computed as the average of y_4, y_5, and y_6.

3. Results and discussion

Our previous alumina-based SERS sensor was fabricated on a round alumina bead (Z) with an average diameter of 4.4 mm. The beads were treated with cetyltrimethylammonium bromide (CTA^+Br^-) to form a CTA^+ bilayer over their surface. The resultant hydrophilic beads (*Z*-$^+$CTACTA$^+$Br$^-$) were treated with 1H,1H,2H,2H-perfluorooctyltriethoxysilane (PFOT) to give PFOT-Z-$^+$CTACTA$^+$Br$^-$ in which PFOT molecules bound to the alumina surface via Al-O-Si bonds and interpenetrated in the CTA^+ bilayers to form hydrophilic niches compartmented by oleophobic-hydrophobic borders. Subsequent treatment with brine replaced the bromide anion in the outer layer of CTAB with chloride (PFOT-*Z*-$^+$CTACTA$^+$Cl$^-$) for the optimal aggregation of citrate-capped silver nanoparticles (AgNPs). Soaking the bead in AgNPs colloid, followed by drying at room temperature, completed the sensor bead (*Z*-CTAB-PFOT-AgNPs). The sampling is conducted by soaking a sensor bead in an aqueous solution of the colorant(s) under study, followed by air-drying. The sensor was then excited on a Raman spectrometer to yield the SERS spectra of the colorant(s). This method was convenient and satisfactory. However, PFOT was not the best choice for building the hydrophilic-hydrophobic gradient due to increasing environmental uncertainty regarding perfluoro compounds [28–31].

To improve the sensor's environmental compatibility, we replaced PFOT with an oil-in-water emulsion of a fluorine-free water repellent (WRP), in which both the WRP molecule and the emulsifiers are derived from natural products. The WRP was applied to compete with the CTA^+Br^- bilayer for the hydrophilic alumina surface, giving WRP-X-*Z*-$^+$CTACTA$^+$Cl$^-$, where X is a surfactant linker. This solid support exhibited the desired bulk surface hydrophobicity (**Fig. S1**) and adsorbent capacity for AgNPs and colorant molecules in the hydrophilic niches (**Fig. S2**). Substituting the bromide anion with chloride using a NaCl solution is optional in this case, since the WRP preparation already contains sufficient chloride anions to achieve this effect.

Further SERS testing with five common food colorants confirmed that the revised sensor beads performed comparably to their PFOT analog (**Fig. S2**). All the colorants except Allura Red gave a distinctive SERS fingerprint. The initial SERS spectrum of Allura Red (2nd spectrum from top, **Fig. S2e**) was uncharacteristic due to strong fluorescence, presumably caused by the local concentration effect of the hydrophilic niche design. The SERS acquired in the solution phase (3rd spectrum from top, **Fig. S2e**, adopted from **Fig. S6a**) showed similar fluorescence interference, though to a lesser extent. The solid bead sensor was preferred in this case for a special operation using a fluorescence absorber, which proved difficult to operate in the liquid phase. Thus, the SERS acquired while the sampled bead was immersed in a 10^{-6} M aqueous solution of methylene blue showed much reduced fluorescence, and a few characteristic SERS bands began to emerge (top spectrum, **Fig. S2e**).

Alumina (aluminum oxide) and chemically modified alumina have been extensively studied as a stationary phase in chromatography [32]. However, it did not affect the fact that silica is used in virtually all commercially available stationary phases, especially in HPLC. Pristine alumina has been found to catalyze the dehydration, decomposition, or isomerization of organic compounds that were being separated on it [33]. Organosilanization is feasible for modifying alumina as a remedy, but has not been utilized substantially to produce a commercial stationary phase. Polymer-coated alumina can be obtained commercially. Only their HPLC performance was not consistently satisfactory.

An alumina stationary phase that doubles as a SERS sensor is possible if the sensor bead fabrication can be replicated on chromatography-grade alumina, further broadening the scope of alumina-based stationary phases. Food colorants are highly polar and water-soluble molecules. The alumina-based sensor is broadly hydrophobic and would be an ideal stationary phase for these hydrophilic analytes. Thus, the chromatography can be reversed-phase using water as the primary mobile phase and minimizing the use of organic solvents, further enhancing the method's environmental benignity. We chose to develop the chromatography method in this work using glass columns since, compared to TLC, column chromatography is amenable to unlimited preparative scale-up (to be reported elsewhere). SERS detection of samples contained in glass capillary tubes has been demonstrated [34–37], implying that in situ SERS detection through glass columns is feasible for achieving sequential separation and detection in a single device.

We applied the revised sensor fabrication process to 1-μm and 10-μm alumina powders (A) to yield A-CTAB-AWRP-AgNPs. Using 10^{-6} M 4-aminophenyl disulfide (APDS) as a SERS probe, we found that both particle sizes performed comparably to their 4-mm bead analog. We packed both sensor powders into individual 15-cm disposable glass Pasteur pipettes as a slurry in water to produce a chromatography column. The 1-μm powder was so fine that it could leak through the bottom cotton plug of the column until it was packed hard, and it drained so slowly when compacted that we ruled it out as the stationary phase. The 10-μm A-CTAB-WRP-AgNPs powder tested satisfactorily and was used as the stationary phase in the following study. **Fig. S3** shows the typical morphologies of the AgNPs (TEM) and 10-μm sensor powder (SEM) used in this study. The AgNPs had an average size of approximately 47 nm. They formed scattered clusters ranging in size from 170 to 670 nm on the alumina surface. Interestingly, EDS showed a low silver content of 0.15–3 atomic % despite satisfactory sensing of APDS. We intended to reduce the flow resistance of the mobile phase [38] by limiting the buildup of the AgNPs layer on the alumina surface. However, the detected silver concentration was lower than expected, with a large % error, presumably because the scanning electrons had knocked out the silver nanoparticles before the detection was complete.

We took two alternative approaches to confirm the effective presence of AgNPs on the alumina powder. First, we repeated the fabrication process with citrate-capped gold nanoparticles (AuNPs) instead of AgNPs. The pink hue of the AuNPs-finished alumina (**Fig. S4b**) was strong evidence for metal nanoparticle adsorption on the alumina powder. In addition to providing indirect evidence supporting the adsorption of AgNPs on the sensor powder, this test suggested a practical advantage of AgNPs over AuNPs for the current purpose. AgNPs-decorated alumina powder, being relatively inconspicuous, provides higher contrast and less visual interference as the background for color analysis.

Second, and more directly, we compared the Raman spectra of APDS on A-CTAB-WRP and A-CTAB-WRP-AgNPs. Fig. 1 shows the Raman spectra of 10^{-6} M APDS on bare alumina powder, A-CTAB-WRP, and A-CTAB-WRP-AgNPs. The Raman signals of APDS were insignificant on

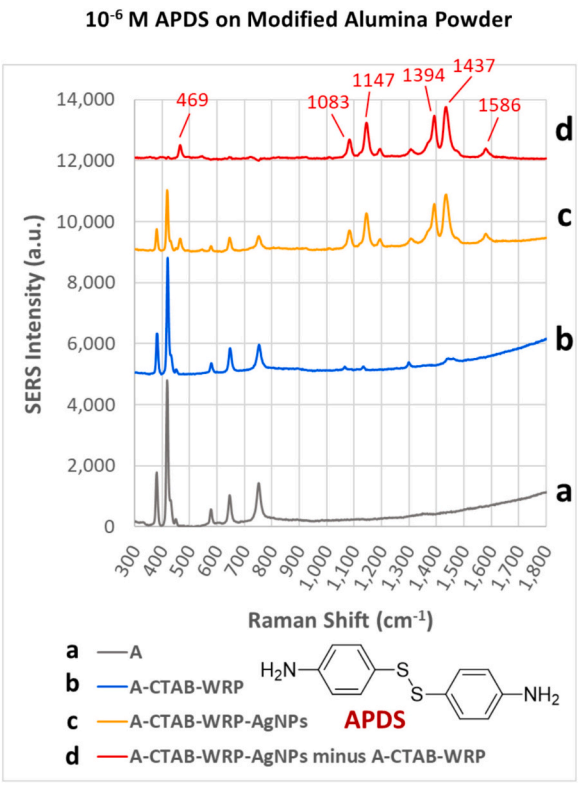


Fig. 1. Raman spectra of 10^{-6} M APDS on (a) A, (b) A-CTAB-WRP, (c) A-CTAB-WRP-AgNPs, and (d) A-CTAB-WRP subtracted from A-CTAB-WRP-AgNPs.

bare alumina powder (Fig. 1a). Similarly, only a few weak signals of the coating were observed on A-CTAB-WRP. Quite the contrary, the spectrum in Fig. 1c, including the bands at 469 (S—S), 1083, 1147, 1394, 1437, and 1586 cm^{-1}, was intense and identical to the SERS fingerprint of APDS [39] [8], indicating the material presence of AgNPs on the alumina surface. A brief study using serially diluted APDS demonstrated that its detectable concentration was as low as 10^{-14} M, as shown in **Fig. S5**. No further dilution was attempted while we proceeded to the major focus of the study.

Two sets of SERS spectra were collected and used as the supporting data for method development. Five popular food colorants served as standards, including Allura Red, Tartrazine, Sunset Yellow, Brilliant Blue FCF, and Indigo Carmine. They were all dissolved in water, as shown in **Fig. S6b**, and their corresponding solution-phase SERS spectra on AgNPs are shown in **Fig. S6a**. The color coatings of a brand-name chocolate candy, including red, yellow, blue, orange, green, and brown, were chosen as the analytes. The candies were soaked in water to dissolve the colorant layer, yielding the solutions in **Fig. S6d**. Their solution-phase SERS spectra (**Fig. S6c**) were then acquired using the same method as the standards. Some features were noted by comparing the two panels of spectra: (1) The SERS of Tartrazine and Indigo Carmine were relatively weak, and Tartrazine's fingerprint was obscure under these conditions. (2) The candy spectra all contained an additional common peak at 729 cm^{-1}. (3) The red candy was primarily colored with Allura Red, blue with Brilliant Blue, and orange with Sunset Yellow. (4) The spectra of Allura Red, as well as the red and brown candies, showed strong fluorescence interference under these detection conditions. We will reveal two additional SERS signatures of Allura Red hereafter, resulting from attempts to resolve this fluorescence issue. (5) The spectra of the yellow candy and tartrazine agreed roughly, which was to be confirmed. (6) The green candy seemed related to both its yellow and blue variants. (7) The brown candy's spectrum consisted predominantly of Allura Red's signature. (8) Deconvolution of the green and brown candy colors was necessary before their formation was determined.

Calibration curves for the five colorant standards were constructed using their UV–Vis absorbance (**Fig. S7**). We estimated that the concentration of the candy-color solutions in **Fig. S6d** was approximately 10^{-4} M using the calibration curves. Hence, 10^{-4} M was set as the standard sample concentration for the subsequent study.

After establishing the procedure of column fabrication and spectra database, 10^{-4} M aqueous solutions of the five colorant standards were loaded into an individual A-CTAB-WRP-AgNPs column. The general retention capacity of A-CTAB-WRP-AgNPs and unmodified alumina columns is demonstrated in **Fig. S8a** using Brilliant Blue as an example. Upon loading, the colorant permeated the unmodified column instantly, but was retained at the top of the A-CTAB-WRP-AgNPs column. After loading, a mobile phase consisting of water and acetone at various ratios was applied to elute the column. A brief test at ambient pressure indicated that the elution was very time-consuming. Thus, we applied pressure to the column using a small aquarium air pump to achieve a flow rate of approximately 6–7 μL/min with 1:1 water-acetone (**Fig. S8b**).

This pressure was sufficient to achieve routine colorant separation within 1–2 h and was safe to apply, considering that the glass column was not pressure-proof by design. The movement of each colorant and dye in the column was visible to the naked eye under these conditions, and any excess mobile phase on top of the stationary phase was removed after the eluted colors had descended a desired distance. The eluted column was placed horizontally on the Raman spectrometer, and the color bands were irradiated for SERS. Typical SERS spectra obtained using this intuitive and concerted procedure are shown in Fig. 2. In general, the SERS spectra were free of solvent interference, agreed well with the corresponding solution-phase SERS (**Fig. S6**), and the SERS fingerprints of Tartrazine and Indigo Carmine were more resolved on the column. Allura Red's fluorescence was again strong (middle spectrum, Fig. 2e) as the colorant was enriched on the column, and a distinct SERS signature was not available under these conditions. In this study, rather than employing fluorescence absorption as in the bead sensor case, we sought to reduce fluorescence interference through photobleaching. Thus, the red band was excited multiple times at the same spot using 100% Laser power, and the top spectrum in Fig. 2e was obtained steadily after three exposures. That said, the structure of the red colorant has been altered photochemically, and this surrogate method should be employed with caution. The fingerprints of the standards from **Figs. S6** (solution) & **2** (VAD-SERS) are summarized in Table 1. This comparison indicated that some peaks observed in the solution data set were absent in the VAD-SERS spectra. Commercial colorant products came with varying levels of purity: Allura Red AC (80%), Indigo Carmine (85%), Sunset Yellow FCF (90%), Brilliant Blue FCF (>97%), and Tartrazine (unspecified). The missing peaks corresponded to the impurities that separated from the color components on the column.

The separation of colors on the A-CTAB-WRP-AgNPs column was tested using three industrial dyes, viz., Red HS, Yellow HGS, and ASMQ (blue). First, 250 μL of a 10^{-4} M aqueous solution of each dye was loaded onto the column and eluted with 600 μL of 1:1 water-acetone to measure their SERS and M_f (migration distance from top of the stationary phase). As shown in Fig. 2f-h, the M_f values were 45 mm (red), 190 mm (yellow), and 220 mm (blue), respectively. Despite the fluorescence interference in Red HS, all three dyes were readily differentiated by SERS.

A stability test of the stationary phase/SERS substrate was also conducted at this point, as follows: Ten A-CTAB-WRP-AgNPs columns were packed and drained until no water was above the stationary phase. They were then placed in a plastic zipper bag and evacuated of air for storage. A column was removed from the bag every week and tested using ASMQ as a probe. The results are shown in **Fig. S9**. The chromatography theoretical number of plates and SERS performance remained comparable until the 7th week, when the blue band started to show signs of diffusion. A crack in the stationary phase was observed in a column between the 7th and 8th weeks. The test with this column showed a

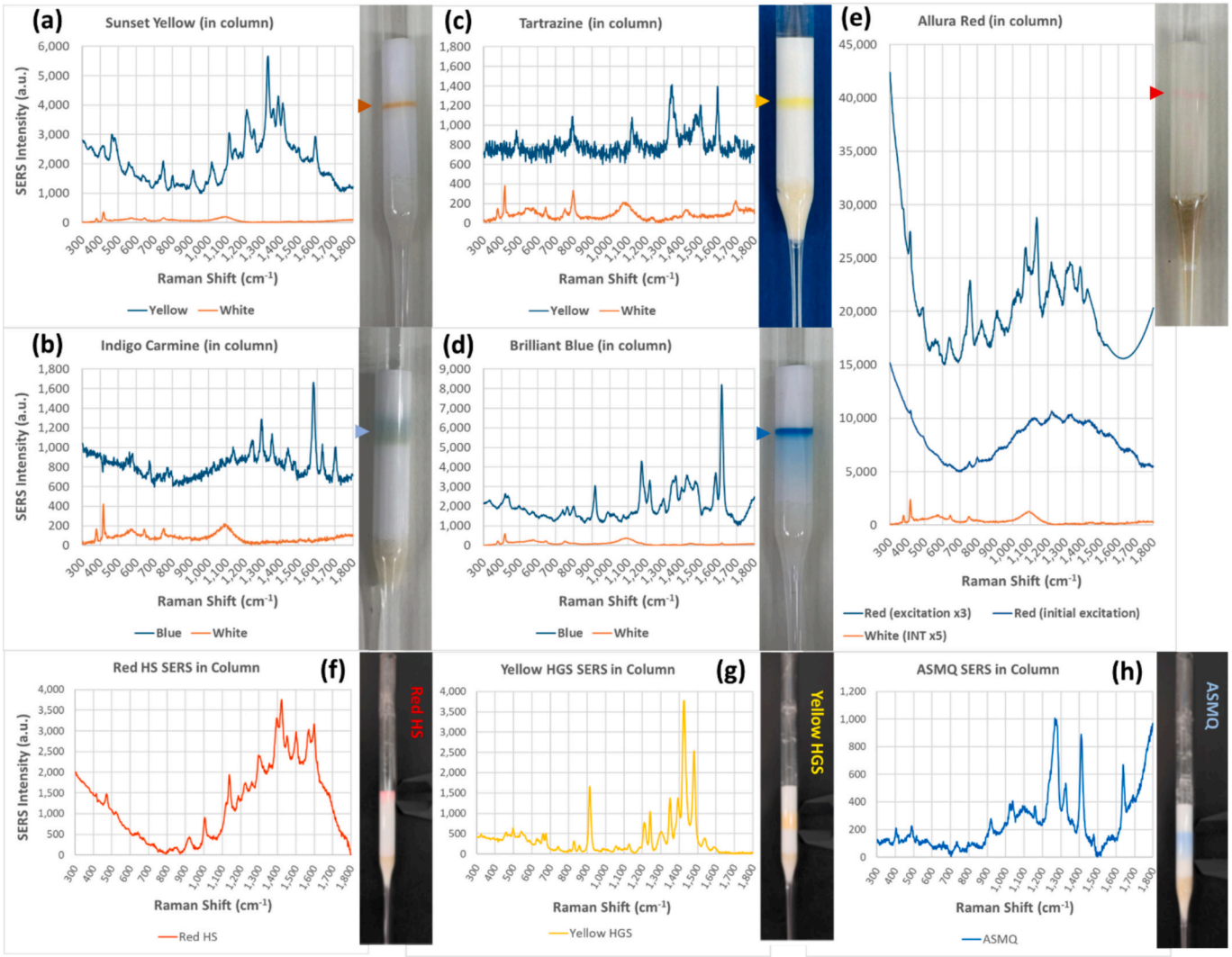


Fig. 2. The column appearances and VAD-SERS spectra of the colorant standards and three industrial dyes: (a) Sunset Yellow, (b) Indigo Carmine, (c) Tartrazine, (d) Brilliant Blue, and (e) Allura Red, (f) Red HS, (g) Yellow HGS, and (h) ASMQ. (For interpretation of the references to color in this figure legend, the reader is referred to the web version of this article.)

diffused band and weaker SERS intensity. It is thus concluded that a packed column remained satisfactory for at least 6 weeks of storage under these conditions.

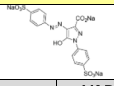
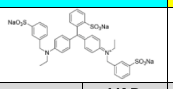
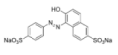
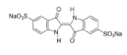
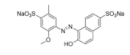
Subsequently, a 1:1:1 mixture (250 μL) of the three dyes, each at a final concentration of 10^{-4} M, was loaded into a new column and eluted with 600 μL of 1:1 water-acetone. Fig. 3 shows the separation and SERS spectra of the colors. Every color band was identified visually and using SERS. Even the green band resulting from the overlapping of yellow and blue colors could be deconvoluted by SERS as a mathematical adduct of Yellow HGS and ASMQ.

Adulteration is a common, often illegal practice in coloring food. A popular method is to displace a legal food colorant with a cheaper industrial dye. The power of VAD-SERS in detecting such adulteration is demonstrated in the following mimic experiment. Three color solutions were prepared by mixing a colorant from the standard collection with an industrial dye of a similar color in a 1:1 ratio: blue with Brilliant Blue and ASMQ, red with Allura Red and Red HS, and yellow with Sunset Yellow and Yellow HGS. The solutions were eluted on their respective A-CTAB-WRP-AgNPs columns using a gradient of H_2O-acetone (*v*/v 1.0:0.2–1.0:0.5) as the mobile phase. This was followed by SERS detection of the separated color bands, as shown in Fig. 4. Each color solution resolved into two bands on the column, evidencing adulteration. The adulterants were quickly characterized by scanning the column with SERS and identified by comparing their spectra with the database.

This established procedure was then applied to analyzing the candy colors. **Fig. S10** shows the column images and SERS spectra of the yellow, blue, orange, and red colorants extracted from the candies. The color renderings were again unambiguously identified as Brilliant Blue for the blue candy and Sunset Yellow for the orange candy. The colorant identity in the yellow candy was not conclusive using solution-phase SERS, as reported previously. It was fully confirmed to be Tartrazine this time using VAD-SERS. In the red candy case, although fluorescence still predominated, the spectrum is identical to that of Allura Red in the column, as shown in the middle section of Fig. 2e. Therefore, no further action was taken regarding the fluorescence, and the hump pattern was considered a VAD-SERS-specific characteristic of Allura Red. Another open issue was the common peak around 729 cm^{-1}, as noted in **Fig. S6c**. This peak was no longer associated with the color bands on the VAD-SERS columns, suggesting the responsible substance is colorless and has been fully separated from the colorants on the column. This substance may be an adjuvant used in candy production, and we decided not to follow up. It suffices to say that the VAD-SERS technique has demonstrated a level of precision that was unparalleled by the solution-phase technique.

We next analyzed the green and brown candy colors using the VAD-

Table 1
The fingerprints of Tartrazine, Brilliant Blue, Sunset Yellow, Indigo Carmine, and Allura Red in the solution and VAD-SERS phases.

Tartrazine		Brilliant Blue		Sunset Yellow		Indigo Carmine		Allura Red	
									
Solution	VAD SERS	Solution	VAD SERS	Solution	VAD SERS	Solution	VAD SERS	Solution	VAD SERS
485	481	420	420	355	349	553	Missing	487	485
1122	1122	741	739	418	415	577	579	635	641
1147	Missing	765	762	467	465	671	671	727	Missing
1311	Missing	804	798	562	557	727	Missing	751	759
1350	1344	919	919	599	Missing	772	774	1032	1035
1502	1501	990	988	633	635	1145	1135	1064	1070
1598	1596	1018	Missing	671	Missing	1243	1241	1096	Missing
--	--	1177	1175	733	737	1271	Missing	1130	1135
--	--	1221	1221	747	749	1295	1293	1223	Missing
--	--	1297	1298	857	Missing	1353	1351	1249	Missing
--	--	1353	1350	899	913	1449	1440	1262	Missing
--	--	1366	1364	934	Missing	1501	Missing	1328	Missing
--	--	1427	1425	988	984	1580	1582	1384	1384
--	--	1474	1474	1032	Missing	1634	1631	1409	Missing
--	--	1488	Missing	1094	Missing	1697	1704	1477	Missing
--	--	1585	1585	1126	Missing	--	--	1502	Missing
--	--	1617	1619	1180	1178	--	--	1547	Missing
--	--	--	--	1230	Missing	--	--	1578	1570
--	--	--	--	1333	1330	--	--	--	--
----	--	--	--	1388	1386	--	--	--	--
--	--	--	--	1418	1411	--	--	--	--
--	--	--	--	1477	1472	--	--	--	--
--	--	--	--	1499	1497	--	--	--	--
--	--	--	--	1547	Missing	--	--	--	--
--	--	--	--	1596	1591	--	--	--	--

SERS technique. The green candy color was separated into yellow and blue bands in the column (Fig. 5a). By comparing the VAD-SERS spectra of the color bands (Fig. 5b) with those of Tartrazine and Brilliant Blue standards (Fig. 5c), the yellow component was identified as Tartrazine and the blue component as Brilliant Blue unambiguously.

The brown candy color was separated into orange, yellow, and blue bands (Fig. 5d). The blue component separated cleanly and was identified as Brilliant Blue by comparing its VAD-SERS spectrum with that of the Brilliant Blue standard (Fig. 5f). The orange and yellow components did not resolve as well as the blue component. The orange component showed the characteristic hump-shaped SERS spectrum of Allura Red. This is analogous to the close similarity between Allura Red and the brown candy in the solution phase (**Fig. S6c**). Thus, the orange band was likely predominantly Allura Red and was tainted by an unseparated yellow colorant to appear orange. Part of the yellow component did not overlap with the red or the blue components and was identified unambiguously as Tartrazine by VAD-SERS. To summarize, the brown candy was rendered using Allura Red, Tartrazine, and Brilliant Blue, or a combination of red and green colors. While the red color was from Allura Red, the green color, also associated with the green candy, was formed by combining Tartrazine (yellow) and Brilliant Blue. The SERS intensity suggested that only a relatively small amount of Tartrazine and Brilliant Blue was used in the brown candy, resulting in a brown color equivalent to green-tinted red. Tartrazine was relatively difficult to detect among the five colorant standards used in this study because it gives low SERS intensity (**Figs. S6a, 2c**). Using the calibration curve in **Fig. S7e**, the concentration of Tartrazine in both the brown and green candy extracts was estimated to be no more than 2×10^{-6} M, equivalent to approximately 0.2 μg of Tartrazine on the column. Doubtlessly, without the effective separation and SERS sensitivity lent by the VAD-SERS technique, identifying a colorant similar to Tartrazine in a mixture of colorants would be highly challenging. It should also be noted that none of the above analyses used more than 1 mL of mobile phase. This makes VAD-SERS an extremely green analytical method.

Finally, a preliminary study (**Fig. S11**) showed that an analytical VAD-SERS column could be used for preparative purposes and recovered >80% of the Brilliant Blue input. This used column also proved reusable, offering the opportunity for recycling if it can be optimized.

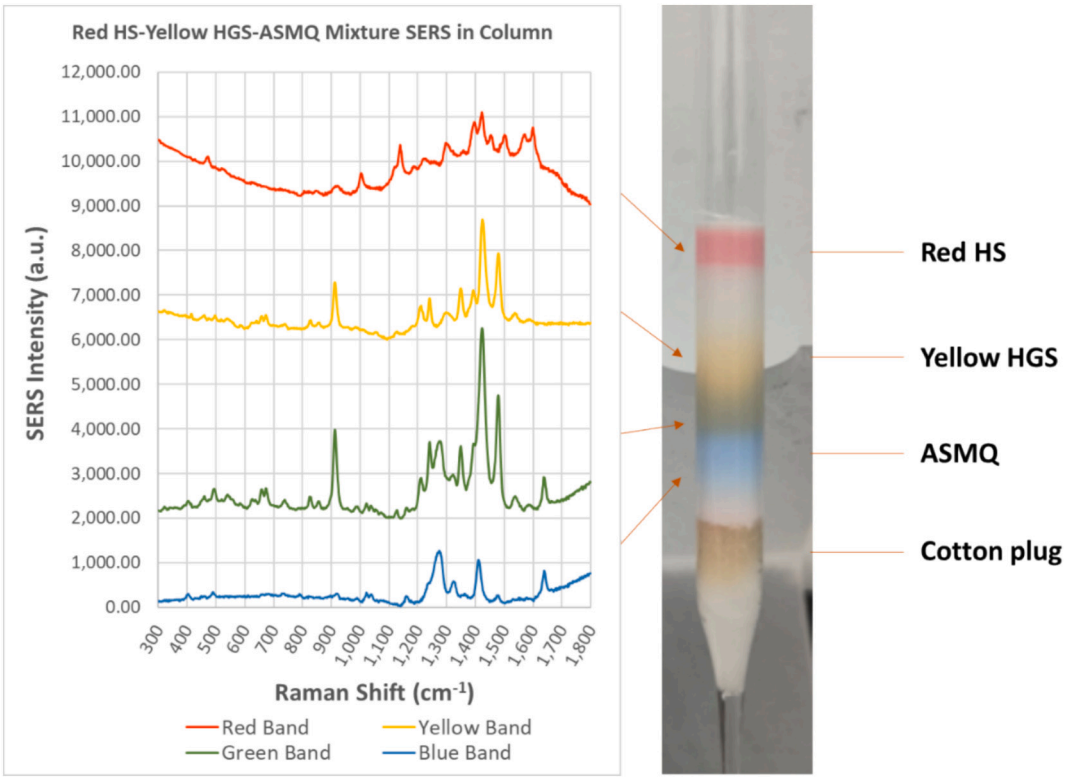


Fig. 3. Chromatography separation and in-column SERS of a 1:1:1 mixture of Red HS, Yellow HGS, and ASMQ. (For interpretation of the references to color in this figure legend, the reader is referred to the web version of this article.)

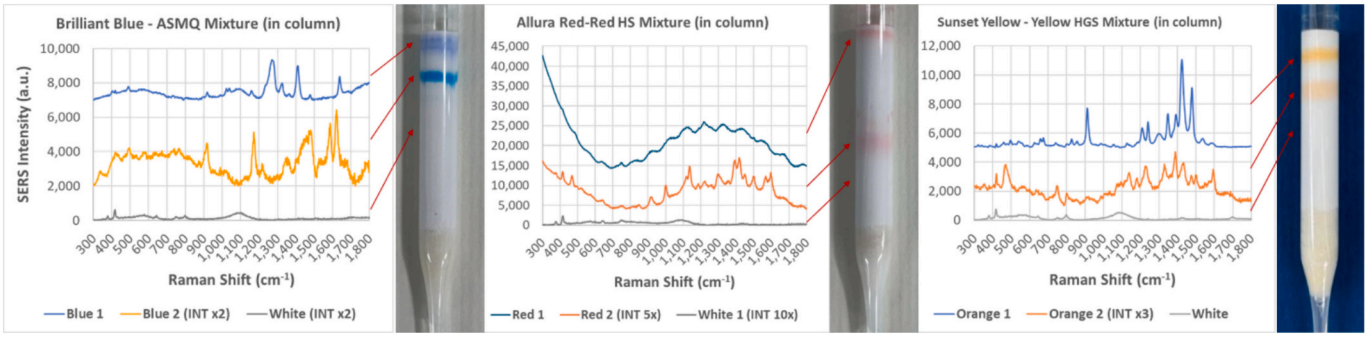


Fig. 4. Separation and detection of mixtures of food colorant-industrial dye that mimic a common practice of color adulteration.

4. Conclusion

Manufactured foods are often colored to arouse consumer interest. The application of colorants to food is a health matter and is regulated by law. While new regulations are being created to tighten the use of food colorants, the development of techniques for analyzing food colors and their illegal uses lags. As such, expensive traditional methods, such as HPLC and MS, were still the best choice. In this study, we developed the VAD-SERS technique to meet this challenge. This innovative method combines the separation efficiency of reversed-phase liquid chromatography with precise, in-situ SERS detection on an alumina-based stationary phase. The fabrication of the SERS sensing stationary phase, even with a designer surface nanostructure and enhanced environmental benignity, is extremely economical and easy. The VAD-SERS analysis procedure is straightforward; elute for separation and excite for SERS using a single column. To demonstrate the versatility of VAD-SERS, we successfully separated a mixture of three industrial dyes and obtained their individual SERS fingerprints on the column. We mimicked food color adulteration by mixing legal food colorants with selected industrial dyes. The VAD-SERS technique successfully resolved the mixtures and identified the mock illegal adulterant. We further demonstrated the power of VAD-SERS in deconvoluting composite colors in real candy samples. A brown candy color was identified as composed of Allura Red and a green tint. The green color was further separated into yellow and blue components, manifested by Tartrazine and Brilliant Blue, respectively.

For comparison purposes, a concise list of earlier techniques that integrated SERS detection with a separation method is presented in **Table S1**. Most of them were not developed for color analysis; some were supported by a model study only, with no proven success on real samples; and many separation methods served only sample pretreatment/enrichment functions rather than chromatography. The efficiency and precision of VAD-SERS make it a highly competitive technique for food safety-oriented color analyses, as demonstrated in this study. It is also a green technique as it uses environmentally friendly materials and requires only a minute amount of water-based mobile phase to complete

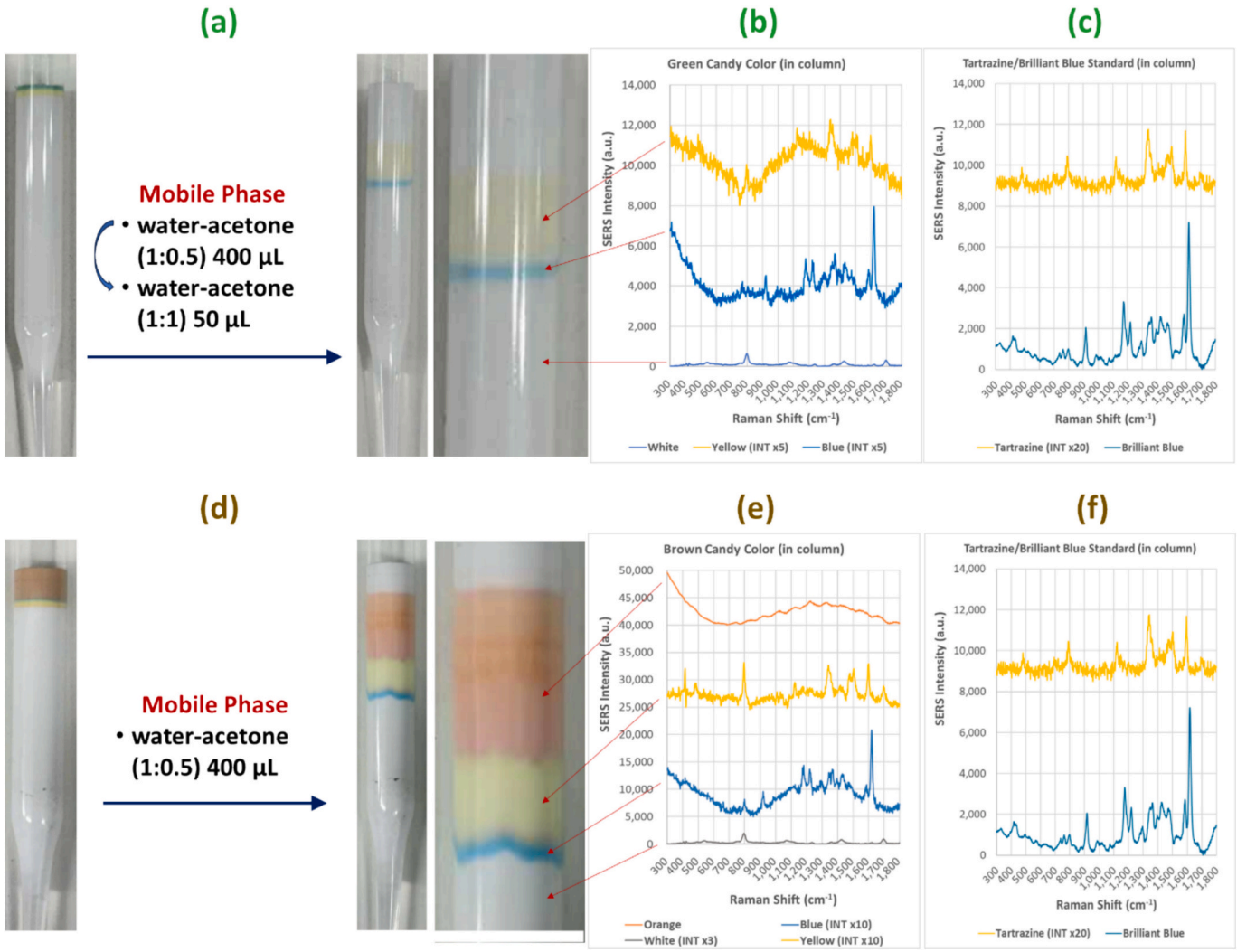


Fig. 5. The analysis of the green and brown candy colors: (a) green candy column before and after elution, (b) VAD-SERS of deconvoluted green candy color, (c) VAD-SERS of Tartrazine and Brilliant Blue standards, (d) brown candy column before and after elution, (e) VAD-SERS of deconvoluted brown candy color, (f) VAD-SERS of Tartrazine and Brilliant Blue standards. (For interpretation of the references to color in this figure legend, the reader is referred to the web version of this article.)

an analysis. Looking forward, this study provides the necessary know-how and background information for ready expansion to a general SERS chromatography. Preparative tasks can be implemented by scaling, and SERS detection for colorless targets can be achieved via Raman mapping [40].

Compliance with ethics requirements

This article does not contain any studies with human or animal subjects.

CRediT authorship contribution statement

Yu-Chi Chen: Investigation, Methodology, Validation. **Ching-Yu Yu:** Investigation, Methodology, Validation. **Hsiao-Ju Yu:** Validation. **Jun Hao Wang:** Software. **Chia-Chi Huang:** Writing – review & editing, Writing – original draft, Visualization, Supervision, Resources, Project administration, Funding acquisition, Formal analysis, Data curation, Conceptualization.

Declaration of competing interest

The authors declare that they have no known competing financial interests or personal relationships that could have appeared to influence the work reported in this paper.

Acknowledgement

The National Science and Technology Council, Taiwan, provided financial support for this work under the project number NSTC-113-2635-M-032-003-MY3. The assistance for SEM analysis from Prof. Trong-Ming Don and Mr. Wei-Ting Kuo of Tamkang University is also appreciated.

Appendix A. Supplementary data

Supplementary data to this article can be found online at https://doi.org/10.1016/j.microc.2026.117923.

Data availability

Data will be made available on request.

References

[1] E. Prabakaran, K. Pandian, Amperometric detection of Sudan i in red chili powder samples using ag nanoparticles decorated graphene oxide modified glassy carbon electrode, Food Chem. 166 (2015) 198–205.

[2] J. Chen, X. Li, A. Huang, W. Deng, Y. Xiao, Nonionic surfactants based hydrophobic deep eutectic solvents for liquid–liquid microextraction of Sudan dyes in tomato chili sauces, Food Chem. 364 (2021) 130373.

[3] N. Wu, W. Gao, Y. Lian, J. Du, X. Tie, The transfer of natural rhodamine b contamination from raw paprika fruit to capsicum oleoresin during the extraction process, Food Chem. 237 (2017) 786–792.

[4] P. Barciela, A. Perez-Vazquez, M.A. Prieto, Azo dyes in the food industry: features, classification, toxicity, alternatives, and regulation, Food Chem. Toxicol. 178 (2023) 113935.

[5] U. FDA, HHS, FDA to Phase out Petroleum-Based Synthetic Dyes in Nation's Food Supply, U.S. Food and Drug Administration (FDA), 2025.

[6] T.R. Ibarra-Rivera, C. Delgado-Montemayor, F. Oviedo-Garza, J. Pérez-Meseguer, V.M. Rivas-Galindo, N. Waksman-Minsky, L.A. Pérez-López, Setting up an educational column chromatography experiment from home, J. Chem. Educ. 97 (2020) 3055–3059.

[7] S. Wang, L. Zhang, Q. Jin, Z. Xu, J. Zhao, Y. Ding, W. Li, P. Lin, J. Gu, Q. Zhang, Y. Chen, H. Chen, T. Yan, Filter paper-based colorimetric analysis: an instrument-free strategy for semiquantitative naked-eye detection of food colorants, Food Chem. 390 (2022) 133087.

[8] Y.-S. Chien, C.-W. Chang, C.-C. Huang, Differential surface partitioning for an ultrasensitive solid-state SERS sensor and its application to food colorant analysis, Food Chem. 383 (2022) 132415.

[9] T.S. Fukuji, M. Castro-Puyana, M.F.M. Tavares, A. Cifuentes, Fast determination of Sudan dyes in chilli tomato sauces using partial filling micellar electrokinetic chromatography, J. Agric. Food Chem. 59 (2011) 11903–11909.

[10] G. Fang, Y. Wu, X. Dong, C. Liu, S. He, S. Wang, Simultaneous Determination of Banned Acid Orange Dyes and Basic Orange Dyes in Foodstuffs by Liquid Chromatography–Tandem Electrospray Ionization Mass Spectrometry via Negative/Positive Ion Switching Mode, J. Agric. Food Chem. 61 (2013) 3834–3841.

[11] G.-W. Jang, S.-I. Choi, S.-H. Choi, X. Han, X. Men, H.-Y. Kwon, Y.-E. Choi, O.-H. Lee, Method validation of 12 kinds of food dye in chewing gums and soft drinks, and evaluation of measurement uncertainty for soft drinks, Food Chem. 356 (2021) 129705.

[12] S. Chen, S. Li, K. Fang, Y. Wang, Y. Yang, C. Han, Y. Shen, Rapid determination of 93 banned industrial dyes in beverage, fish, cookie using solid-supported liquid–liquid extraction and ultrahigh-performance liquid chromatography quadrupole orbitrap high-resolution mass spectrometry, Food Chem. 388 (2022) 132976.

[13] W. Zhou, X. Wang, Y. Liu, W. Zhang, X. Di, Novel cu2+−based immobilized metal affinity magnetic nanoparticles for fast magnetic solid-phase extraction of trace Sudan dyes in food samples, Food Chem. 404 (2023) 134432.

[14] H. Awad, M.M. Khamis, A. El-Aneed, Mass spectrometry, review of the basics: ionization, Appl. Spectrosc. Rev. 50 (2015) 158–175.

[15] M. Beneito-Cambra, B. Gilbert-López, D. Moreno-González, M. Bouza, J. Franzke, J. F. García-Reyes, A. Molina-Díaz, Ambient (desorption/ionization) mass spectrometry methods for pesticide testing in food: a review, Anal. Methods 12 (2020) 4831–4852.

[16] A. Beganović, L.M. Hawthorne, K. Bach, C.W. Huck, Critical review on the utilization of handheld and portable raman spectrometry in meat science, Foods 8 (2019) 49.

[17] A. Synytsya, Z. Kováčová, D. Janstová, M. Vočka, J. Petrtýl, L. Petruželka, Comparative study on handheld, modular, and laboratory raman instruments for the analysis of colon tissues and colorectal polyps, Appl. Sci. 14 (2024) 791.

[18] V. Peksa, M. Jahn, L. Štolcová, V. Schulz, J. Proška, M. Procházka, K. Weber, D. Cialla-May, J. Popp, Quantitative SERS analysis of azorubine (e 122) in sweet drinks, Anal. Chem. 87 (2015) 2840–2844.

[19] Y.-j. Ai, P. Liang, Y.-x. Wu, Q.-m. Dong, J.-b. Li, Y. Bai, B.-J. Xu, Z. Yu, D. Ni, Rapid qualitative and quantitative determination of food colorants by both raman spectra and surface-enhanced raman scattering (SERS), Food Chem., 241 (2018) 427–433.

[20] N.R. Barveen, T.-J. Wang, Y.-H. Chang, Z. Yuan-Liu, Ultrasensitive and reusable SERS probe for the detection of synthetic dyes in food industry through hybrid flower-shaped ZnO@ag nanostructures, J. Alloys Compd. 861 (2021) 157952.

[21] L. Tan, Y. Cao, J. Yan, K. Mao, L. Liu, X. Wang, W. Ye, R.A. Harris, H. Zhang, TiO2 nanorod arrays@PDA/ag with biomimetic polydopamine as binary mediators for duplex SERS detection of illegal food dyes, Anal. Chim. Acta 1287 (2024) 342047.

[22] N.R. Barveen, C.-W. Zeng, Y.-W. Cheng, Machine learning-integrated SERS platform based on AuSe nanowires for indigo carmine detection in real samples, Food Chem. 494 (2025) 146120.

[23] C.-C. Huang, C.-H. Huang, I.T. Kuo, L.-K. Chau, T.-S. Yang, Synthesis of silica-coated gold nanorod as raman tags by modulating cetyltrimethylammonium bromide concentration, Colloids Surf. A Physicochem. Eng. Asp. 409 (2012) 61–68.

[24] C.-C. Huang, W. Chen, A SERS method with attomolar sensitivity: a case study with the flavonoid catechin, Microchim. Acta 185 (2018) 120.

[25] Z.-H. Hsu, L. Hsu, C.-C. Huang, Polyacrylamide gel scaffold immobilized with silver nanoparticles as SERS substrates and catalysts for h2 generation via methanolysis of NaBH4, ACS Appl. Nano Mater. 5 (2022) 2258–2265.

[26] Y.-S. Hung, C.-W. Chang, Y.C. Shen, Y.-C. Yu, W.-L. Huang, C.-C. Huang, Spectroscopic analyses of particle and energy aggregations at the interface of silver nanoparticles and fluorescent carbon nanodots, Nanoscale 15 (2023) 13987–13996.

[27] P. Ravisankar, V. Swathi, P. Srinivasa Babu, G. Shaheem Sultana Md, Current trends in performance of forced degradation studies and stability indicating studies of drugs, IOSR J. Pharm. Biol. Sci. 12 (2017) 17–36.

[28] T. Stahl, D. Mattern, H. Brunn, Toxicology of perfluorinated compounds, Environ. Sci. Eur. 23 (2011) 38.

[29] A.F. Peritore, E. Gugliandolo, S. Cuzzocrea, R. Crupi, D. Britti, Current review of increasing animal health threat of per- and polyfluoroalkyl substances (PFAS): harms, limitations, and alternatives to manage their toxicity, Int. J. Mol. Sci. 24 (2023).

[30] Z. Habib, M. Song, S. Ikram, Z. Zahra, Overview of per- and polyfluoroalkyl substances (PFAS), their applications, sources, and potential impacts on human health, Pollutants 4 (2024) 136–152.

[31] H. Brunn, G. Arnold, W. Körner, G. Rippen, K.G. Steinhäuser, I. Valentin, PFAS: forever chemicals—persistent, bioaccumulative and mobile. Reviewing the status and the need for their phase out and remediation of contaminated sites, Environ. Sci. Eur. 35 (2023) 20.

[32] J.J. Pesek, M.T. Matyska, Modified aluminas as chromatographic supports for high-performance liquid chromatography, J. Chromatogr. A 952 (2002) 1–11.

[33] Q.-W. Zhang, L.-G. Lin, W.-C. Ye, Techniques for extraction and isolation of natural products: a comprehensive review, Chin. Med. 13 (2018) 20.

[34] Q. Jiang, T. Zeng, S. Yang, Q. Chen, L. Chen, Y. Ye, J. Zhou, S. Xu, On-column enrichment and surface-enhanced raman scattering detection in nanoparticles functionalized porous capillary monolith, Spectrochim. Acta A Mol. Biomol. Spectrosc. 141 (2015) 244–251.

[35] Y. Pan, X. Wang, H. Zhang, Y. Kang, T. Wu, Y. Du, Gold-nanoparticle, functionalized-porous-polymer monolith enclosed in capillary for on-column SERS detection, Anal. Methods 7 (2015) 1349–1357.

[36] W.F. Nirode, G.L. Devault, M.J. Sepaniak, R.O. Cole, On-column surface-enhanced raman spectroscopy detection in capillary electrophoresis using running buffers containing silver colloidal solutions, Anal. Chem. 72 (2000) 1866–1871.

[37] L. Fan, Z. Wang, Y. Zhang, Y. Song, H. Yang, F. Wang, Molecularly imprinted monolithic column-based SERS sensor for selective detection of cortisol in dog saliva, Talanta 249 (2022) 123609.

[38] T. Edge, Chapter 4 - turbulent flow chromatography in bioanalysis, in: I.D. Wilson (Ed.), Handbook of Analytical Separations, Elsevier Science B.V., 2003, pp. 91–128.

[39] H.E. Van Wart, A. Lewis, H.A. Scheraga, F.D. Saeva, Disulfide bond dihedral angles from raman spectroscopy, Proc. Natl. Acad. Sci. U. S. A. 70 (1973) 2619–2623.

[40] F.W.L. Esmonde-White, M.D. Morris, Raman Imaging and Raman Mapping, in: P. Matousek, M.D. Morris (Eds.), Emerging Raman Applications and Techniques in Biomedical and Pharmaceutical Fields, Springer Berlin Heidelberg, Berlin, Heidelberg, 2010, pp. 97–110.